PORE CHARACTERISATION, RELATING MINI-PERMEABILITY AND CT-SCAN POROSITY OF CARBONATE CORES

M.T. Tweheyo[1], A.S. Lackner[2], G.K. Andersen[2], J.K. Ringen[3] and O. Torsaeter[2]
[1]Stavanger University, [2]Norwegian University of Sci. & Tech., [3]STATOIL

This paper was prepared for presentation at the International Symposium of the Society of Core Analysts held in Toronto, Canada, 21-25 August 2005

ABSTRACT

This work was performed on two reservoir carbonate cores. The objectives were to: (i) determine possible functional permeability/porosity relationship at various sampling scales, and (ii) characterise the rocks with respect to mineralogy, pore size distribution and geometry. Scaling was based on mini-permeameter data obtained at cross-section surfaces and along whole cores, and on porosity data contained in computer-tomography (CT)-scan images each comprising a cross-section of 414x414 values. The other available data included air permeability and Helium porosity on samples of varying size: whole cores, SCAL plugs- and 1-inch plugs. By overlaying the CT images to the corresponding end-face mini-permeability matrix, we sought to determine permeability/porosity correlations at various scales. Pore characterisation was based on thin sections, mercury porosimetry, backscattered electron images (BSE) and X-ray elemental maps obtained from combined scanning electron microscopy (SEM). The analyses revealed highly heterogeneous rocks with wide range of pore sizes that should be described by bi-modal distribution function. The mineralogy showed that core 1 had more calcite with thin layers of calcite cement aligning the pore walls while core 2 was more dolomatized and relatively homogeneous.

INTRODUCTION

To understand fluid distribution and flow in porous media, it is essential to have an improved description of the media properties from a representative sample and sampling scale. The key petrophysical properties are usually determined by core analysis or logging. Many published results in the literature on sandstone show strong correlation between porosity and permeability with positive slope [1]. However, such reliable correlations are uncommon in carbonates and even with most sandstones, the correlations are subject to severe limitations and are seldom used. One such limitation is that statistically, both core analysis and logging provide inadequate sampling of porosity and permeability data.

This work is an attempt to relate permeability and porosity of carbonate samples based on whole core data and detailed small-scale mini-permeability and various scales of

porosity data. Traditionally, mini-permeameter data have been applied in reservoir characterisation through quantification of small-scale heterogeneities and their influence on fluid flow, and for assigning more realistic permeability values to grid-blocks in simulation studies. Here, we assess the applicability of the method in establishing a porosity/permeability relationship by statistically acquiring more data values from a core grid (Figure 1). An advantage of this method is that sampling can be carried out virtually anywhere on the rock surface and the technique has been successfully used to explore small-scale variations on outcrop surfaces and cores [2-4]. Pore scale studies were also performed to provide better understanding of the samples, particularly regarding the geology and heterogeneity.

MATERIALS AND METHODS

Two reservoir cores containing 68 and 52 cross-sectional CT scans with 414x414 porosity values each, along with the core depths, were available for core 1 and 2, respectively. The mini-permeameter included 4 data sets from each half-core end-face represented by a 10x10 square matrix with sides of 5.85 cm, local permeabilities measured along the slab, and Helium porosities from whole cores, SCAL plugs and 1-inch plugs - Figure 1(a) and (b). The CT-image corresponding to a particular end-face permeability matrix was found and then oriented to exactly overlay the permeability grid. Then the porosity matrix was reduced to the physical size of the mini-permeameter grid and the data correlated.

Mercury porosimetry was done on two samples from each core which were stored at 60˚C before evacuation to constant weights. The data were used to calculate the pore size distribution as a function of pore and throat radii [5]. The pores were characterised by their relative pore volume contributed by pores with throat radius $r_{i.}$ The capillary pressure function for a cylindrical tube of radius r_i was related to a pore distribution function $D(r_i)$ by Equation (1), where $D(r_i)\Delta r_i$ is the fraction of the pore volume contributed by pores with radius between r_i and $(r_i + \Delta r_i)$, and S is air saturation [1]. The experimental mercury data were de-noised and the discrepancy between data points removed by a moving average and smoothing routine. Pore size distribution curves and indexes were generated from pore volume and pore size data, and intrusion capillary pressure data, respectively.

$$D(r_i) = \frac{\Delta\phi}{\Delta r_i} = \frac{P_c}{r_i}\frac{dS}{dP_c} . \qquad (1)$$

Two thin sections from each core were characterised by SEM combined with an EDS (Energy Dispensive Spectrometer) X-ray interpreter. They were polished, impregnated by an epoxy and then coated with carbon to create an electronic conductive surface. X-ray images with 512x352 pixels and BSE images with 1024x704 pixels were produced by an accelerating voltage of 10 kV to excite the mineral elements. The bulk- and pore-wall mineralogy was based on quantitative analysis of the SEM images (elemental maps).

RESULTS AND DISCUSSIONS

Mini-permeameter and CT-scans correlations

The whole core data is shown in Figure 1(c) while the Helium porosity, CT scan mean porosity and slab permeability vs. depth are shown in Figure 2. The figures reveal considerable but homogeneous spread in the local porosities over the cores. Figure 3 shows the permeability vs. porosity for the slab of core 1 (a), and the end-face values of core 2 (b). The variation is random and the spread between the averaged mini-permeameter data and porosities is large. The CT porosities covering the mini-permeameter area (241x241 grid) were further reduced to 10x10 grid and then averaged to 5x5 grids but showed no improved correlation at both scales. The general trend shows a small spread in porosity and a large variation in the spatial permeability. Most carbonate reservoirs have complex diagenetic history involving early compaction and porosity loss followed by an episode of porosity generation associated with thermal karstification [6]. Such heterogeneities at reservoir and micro levels cause significant variation in permeability and porosity making correlation difficult and these parameters should be measured on whole core samples.

Thin sections: geological interpretation

The geological interpretation is based on image processing and visual observations through a microscope. Core 1 is a bioclastic limestone consisting of long fibrous shell fragments, microfossils, micritic lime mud, and has thin layers of calcite cement aligned along the pore walls. Accordingly, this is a packstone consisting of fossil grains and fragments [7]. Core 2 is a mono-mineral rock with rhombohedral-microfossil grains. The rock might originally have been an oolithic limestone composed of ooids, i.e, ellipsoidal or spherical bodies with a nucleus and radial structure grown in a turbulent environment. It is more homogeneous and the textural details show strong dolomatization. The pore system in both cores is highly irregular and complex revealing increased heterogeneity.

Mercury porosimetry: pore size distribution and geometry

The volume-pressure curves shown in Figure 4 reveal substantial trapping of Hg. The bioclastic limestone core 1 has larger pores than the highly dolomatized core 2. These characteristics were interpreted as bi-modal pore distribution consisting of spherical and cylindrical (or conical) shapes. Due to the narrow access between pores in a spherical model, pore filling is slow and the intrusion curve very steep. A lot of mercury is retained during the extrusion process causing large hysteresis. On the other hand, intrusion curves in conical pore models have more or less flat slopes and Hg penetration increases according to pressure and the hysteresis is small. The data show large hysteresis with spherical pores probably dominant. The gentle, increasing penetration curves indicate strong heterogeneity with non-uniform and wide range of pore sizes.

The curve shapes in Figure 5(a) show bigger pore volumes per gram in core 1 than in core 2, which is consistent with the porosities in Table 2. Figure 5(b) shows bi-modal

peaks from the de-noised, averaged and smoothed pore size distribution based on derivatives of the volume curves using Equation (2). The volume contribution from the small pores is much lower and the distribution is not distinctly asymmetric but has a tail towards the lower pore size ranges. Core 1 shows a wider pore size distribution and increased heterogeneity than core 2, which is relatively homogeneous as observed from the images.

$$\frac{dV_m}{d\log(r_m)} = \frac{V_{m,i+1} - V_{m,i}}{\log(r_{m,i}) - \log(r_{m,i+1})} \qquad (2)$$

Figure 6 shows logarithmic plots of capillary pressure (P_c) and effective saturation (S_w) while the distribution indexes are given in Table 1. A large index is associated with uniform pore size distribution and is common in unconsolidated natural sandstones and some limestones. Accordingly, the values show slightly less uniformly distributed pores in core 1 than core 2, which is consistent with observations from the thin sections. Generally, however, the low indexes indicate very wide range of pore sizes in both rocks. The figure also demonstrates the trapping and capillary hysteresis phenomenon observed earlier.

Mineralogy

The key mineral elements in Table 1 show higher Ca content and $CaCO_3$ ratio in core 1 than core 2. Understanding of calcite distribution is important because it can directly influence the cementing and fluid flow properties. The high occurrence of Mg in core 2 is consistent with the dolomatization observed before. High resolutions show traces of silica and thin layers of mainly calcite (dark grey) aligning the pore walls in core 1 (Figure 7). Pore wall mineralogy is important to describe petrophysical parameters that depend on mineralogy by considering the mineral proportions in direct contact with the pore fluid.

SUMMARY

Heterogeneous carbonates should have porosity and permeability measured on whole core samples. Probe permeability measurements need to be made at very close spacings and the results evaluated with other methods such as whole core analysis, CT scanning and thin section studies. CT scans are very useful in calibrating porosity values for selected samples. Mercury injection data should be used to determine pore size distribution for all rock types, and also to determine if bi-modal models should be used. Pore wall studies add value to rock typing and petrophysical response evaluation.

ACKNOWLEDGEMENT

The authors would like to acknowledge STATOIL for the material and financial support.

REFERENCES

1. Chierici, G.: "Principles of Petroleum Engineering," (1994) Vol. 1.
2. Dyer, T., Scheie, A., and Walderhaug, O.: "Mini-permeameter-Based Study of Permeability Trends in Channel Sand Bodies", *AAPG Bull.* (1990) 74.
3. Jensen, J.: "A Model for Small-Scale Permeability Measurements With Applications to Reservoir Characterisation", *SPE/DOE 20265 pres. at the SPE/DOE Symp. on EOR*, Tulsa (Apr. 22-25, 1990).
4. Cobbert, P., and Jensen, J.: "A Comparison of Small Scale Permeability Measurement Methods for Reservoir Characterisation", *paper pres. at the 1991 Conf. on Adv. in Res. Tech*. Edinburgh (Feb. 21-22).
5. Salmas, C., and Androutsopoulus, G.: "Mercury Porosimetry: Contact Angle Hysteresis of Materials with Controlled Pore Volume," *J. Colloid Interface Sci*. (2001) 239, 178-189.
6. Alpin, G., and Sapru, A.: "Characterisation of Carbonate Reservoir Heterogeneity Using Probe Permeability Images, Petrography and Borehole Image Log Data", *paper SCA 2001-41, Proc. Int. Symp. Of the Society of Core Analysts*, Edinburgh, (Sept. 17-19, 2001).
7. Scholle, P.: "Carbonate Rock Constituents, Textures, Cements & Porosities," *AAPG Memoir* 27 (1978).

Table 1—Key rock parameters and mineral components.

Parameter	**Core 1**		**Core 2**	
Sample	1.1	1.2	2.1	2.2
Pore size distribution index, λ	0.605	0.531	0.690	0.618
Mg, wgt %	0.301	0.314	8.385	7.43
Ca, wgt %	25.346	30.045	15.696	14.588
$CaCO_3$:SiO_2:MgO	757:10:2	937:10:2	126:10:5	487:10:2

Table 2—Whole core data measurements

Plug description	**Core 1**			**Core 2**		
	Number	ϕ_{He}	K_{Kl}	Number	ϕ_{He}	K_{Kl}
Whole core	1W	0.209	11.8	2W	0.180	12.90
Vertical 1.5 inch (SCAL)	1.1VS	0.212	20.5	2.1VS	0.160	7.52
Vertical 1.5 inch (SCAL)	1.2VS	0.203	9.12	2.2VS	0.171	7.08
Vertical 1 inch	1.1V	0.221	34.3	2.1V	0.161	7.71
Vertical 1 inch	1.2V	0.208	7.98	2.2V	0.162	2.82
Horizontal 1 inch	1.1H	0.195	17.3	2.1H	0.183	71.30
Horizontal 1 inch	1.2H	0.198	8.01	2.2H	0.178	29.60

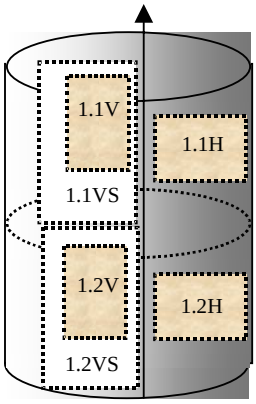

Figure 1(a): Whole cores

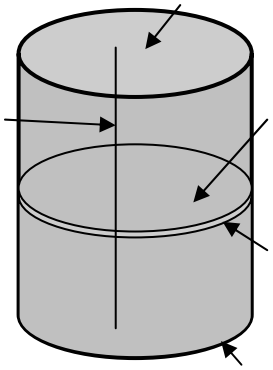

Figure 1(b): Probe permeability grids: 4 surfaces and 1 stack

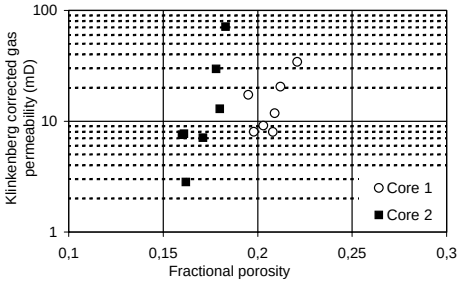

Figure 1(c): Permeability vs. porosity data from whole cores

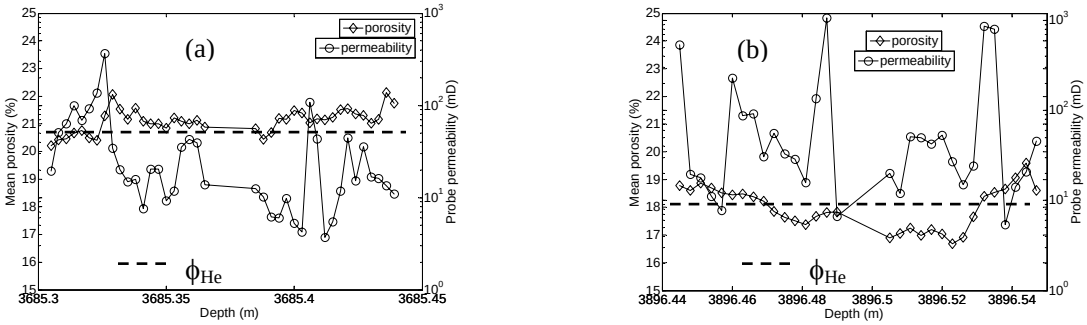

Figure 2—Mini-permeability and CT porosities vs. depth: (a) core 1, and (b) core 2.

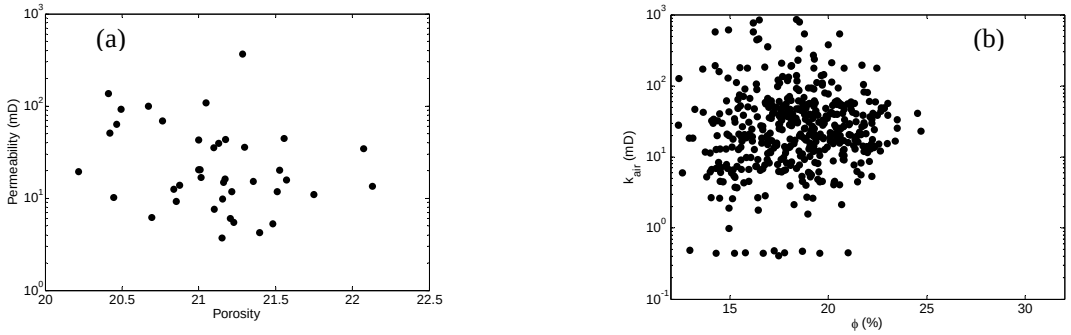

Figure 3—Permeability vs. porosity based on 10x10 grids: (a) core 1, and (b) core 2.

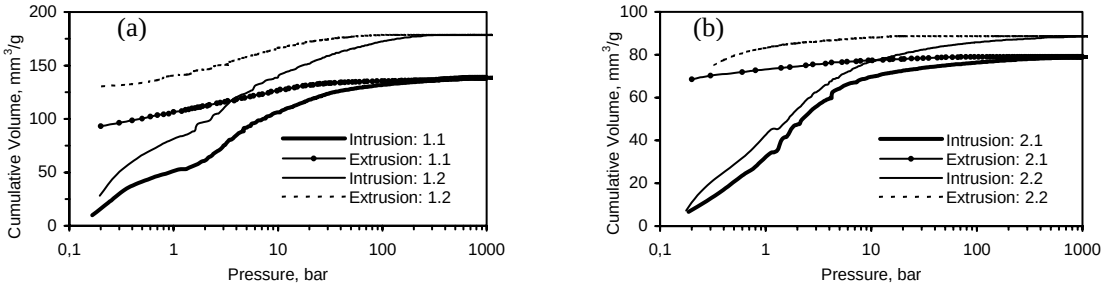

Figure 4—Mercury intrusion and extrusion data for (a) core 1 and (b) core 2.

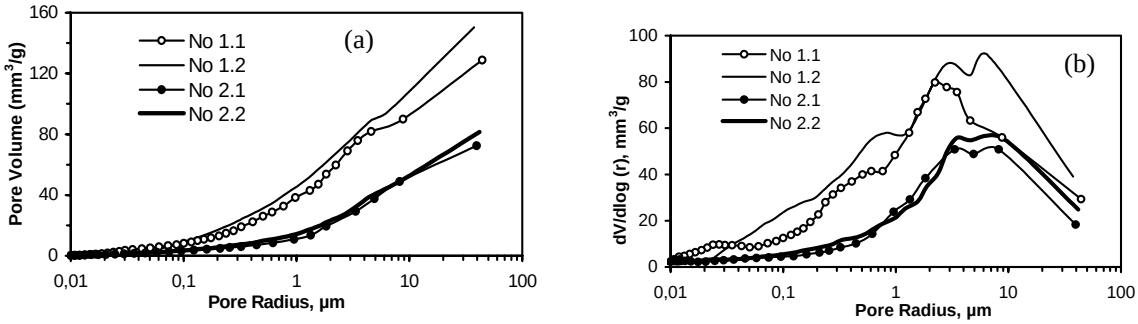

Figure 5—(a) Cumulative pore volume, and (b) pore size distribution derivative curves.

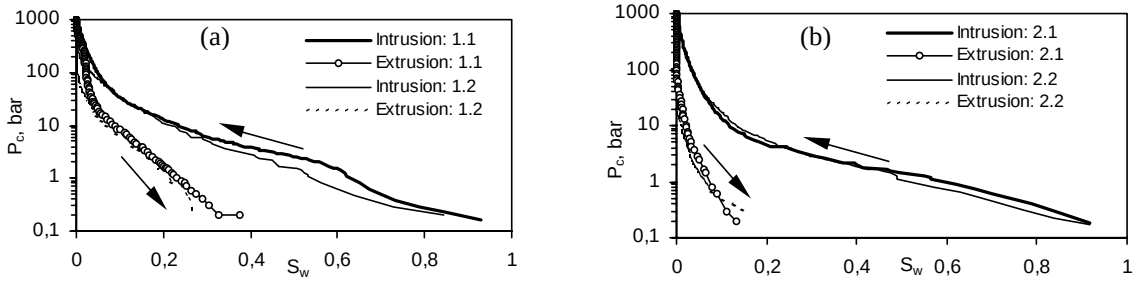

Figure 6—Hysteresis effects in capillary pressure for (a) core 1 and (b) core 2.

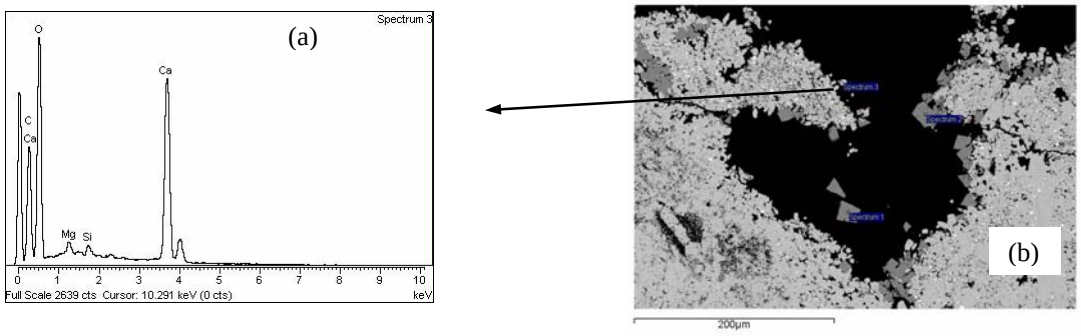

Figure 7—(a) Pore wall mineralogy spectrum, and (b) X-ray image (X800) from core 1.